



Optimizing Weight Percentage of MWCNTs for Enhancing LVI Resistance of Quasi-Isotropic Symmetric Laminate of Carbon Woven Fabric/ Epoxy Embedded with MWCNTs

P. Rawat^{1,2} · K.K. Singh² · N.K. Singh³ · S. K. Tiwari⁴ · A. Sharma⁵

Received: 4 December 2017 / Accepted: 22 May 2019 / Published online: 10 June 2019
© The Society for Experimental Mechanics, Inc 2019

Abstract

This research work investigates the energy absorption, and damage tolerance behavior of three phased (carbon woven/epoxy/multiwall carbon nanotubes) polymer composites. Five doping weight fractions of multi-wall carbon nanotubes (MWCNTs) are considered as 0, 1, 2, 3 and 4 wt.% of thermosetting epoxy resins. Low-velocity impact (LVI) tests are conducted on drop tower setup with three different velocities, 3.5, 4.5 and 5.5 m/s. Damage caused by a 10 kg, hemispherical headed cylindrical impactor is analyzed and compared. The experimental results showed an increase in the energy absorption up to 3 wt.% of the MWCNT doping. However, reinforcing above this percentage, the energy absorption is reduced due to the formation of MWCNT agglomerations. Therefore, this work proposed an optimized doping percentage for CFRP laminates. The maximum improvement of 51.83% in energy absorption was found at 3 wt.% of MWCNT reinforcement in epoxy resins.

Keywords Impact testing · MWCNT · Three-phased composite · Energy absorption

Introduction

Over the last five decades, fiber reinforced polymer (FRP) composites have been used extensively in several advanced industrial components like wind turbine blades [1–3]. This use is still growing continuously due to specific features offered by the FRPs like high strength and stiffness ratio to its weight and design flexibility. However, woven fiber (Glass, Carbon, Kevlar fiber, etc.) polymer composites are used in industries, where high strain rates and/or impact loading is a grave concern [4–6]. In this regard, FRPs offer brittle fracture behavior

as compared to metals with ductile nature. However, these limitations of the matrix can be overcome by using secondary reinforcement [7] in woven composites. Four basic mechanisms, (i) matrix cracking, (ii) crack growth, (iii) delamination and (iv) fiber failure or breakage [8], take place when FRP goes under impact loading. Many studies have reported the improvement in impact response of FRPs using several techniques as design aspect [9–11], hybrid composite [12–15], sandwich structures [16, 17] and nano-fillers as secondary reinforcement [18–20].

Iijima [21] discovered carbon nanotubes (CNTs) in 1991. These nanotubes attracted the interest of research community due to their specific mechanical, thermal and electrical properties. Schadler et al. [22] studied the load transfer characteristics of nanotubes epoxy composites and concluded a significant improvement in tensile and compressive modulus. Also justified that compression modulus (6.0 MPa) is higher than tensile modulus (4.2 MPa) in CNT/epoxy composite using multiwall carbon nanotubes at 5 wt.% of reinforcement. Karapappas et al. [23] analyzed fracture properties of MWCNTs doped CFRP composites and found MWCNTs as an ideal reinforcement for polymer-based composites. This research reported about 60% increase in fracture energy at 1 wt.% of nanotube doping. Davis et al. [24] examined improvement in mechanical properties of CFRP laminates using f-CNT and reported 18% increase in strength, 24%

✉ P. Rawat
aadiprashant@gmail.com

¹ College of Civil Engineering, Hunan University, Changsha 410082, China

² Department of Mechanical Engineering, Indian Institute of Technology (ISM), Dhanbad 826004, India

³ Mechanical Engineering Department, School of Engineering, Dayananda Sagar University, Bangalore 560078, India

⁴ Mechanical Engineering Centre, Hanyang University, Hanyang 04763, South Korea

⁵ Alliance College of Engineering and Design, Alliance University, Bangalore 560068, India

enhancement in stiffness at 0.5 wt.% f-XD-CNT materials and 42% improvement in material durability (T-T loading test) at 0.3 wt.% reinforcement.

Damage mechanism characterization [25] of fiber reinforced composite reported about the close relation of resin toughness over impact damage resistance. The work concluded significant improvements in energy absorption by changing ply orientations, minimum damage occurrence on the impacted side while maximum damage on opposite side occurs due to peeling stress. Siegfried et al. [26] modified resins using three different types of carbon nanotubes to investigate the impact and post impact effects. This experimental study concluded that CNT network has a positive influence on the FRP properties. Moreover, investigation of MODE II failure zone reported about the presence of MWCNTs everywhere, and agglomerations of CNTs were observed for aged carbon nanotubes. The presence of carbon nanotubes were seen at rich resin zones which was the main cause of agglomerations. Koricho et al. [27] studied the behavior of pristine and nano-micro modified glass/epoxy composite under LVI testing. In this investigation, 1 wt.% nano-clay (NC) doped specimen absorbed maximum energy followed by a micro-glass bubble (GB), hybrid and neat GFRP laminates. Gonzalez et al. [28] also performed similar tests using short carbon fiber reinforced (SCFR) PEEK composites using experiments and numerical simulations. The work proposes for failure prediction, i.e., homogenization and elastic materials and anisotropic damage. The work state about the decrease in energy absorption capabilities in unmodified PEEK.

The above review proves that the presence of nanoparticles improves the impact damage tolerance of polymer composites. Moreover, impact is a daily life situation that commonly occurs [4, 7], much attention (by previous researchers) have been focused on the enhancement in impact properties by modifying resins using nanofibers and/or CNTs. This improvement varies with the doping percentage, but with the increase in doping percentage in resin after certain value advances in material properties stops and starts decreasing [11]. Only a few researchers have considered this issue, while most of the research work investigates about reporting improvement at random doping values.

Tehrani et al. [29] experimentally explored mechanical behavior and impact damage assessment using MWCNTs and concluded about 21% energy absorption increment at 2 wt% doping. Kostopoulos et al. [20] examined the impact and after impact characteristics of 0.5 wt.% of MWCNT embedded CFRP composite. The work highlighted about no significant effect of doping on low energy impacts while with the increase in drop energy difference in laminate performance increases and modified CFRP laminate absorbed more energy as compared to neat samples. For after impact testing strength and compressive modulus for modified samples were also improved. In previous work, Singh et al. [11] observed a

decrease in energy absorption value at 5 wt% but at 2 wt.% this energy absorption was found to be maximum, i.e., 13.53%, but in this study, no optimum value for maximum energy absorption was proposed. Similarly, Soliman et al. [30] used variation in MWCNT reinforcement percentage as neat epoxy, 0.5%, 1.0% and 1.5% of resins and reported about the increase in energy absorption with the growth in doping percentage. Experimental investigation justified about 50% increase in energy absorption at 1.5% doping. However, these investigation did not propose any optimum value for maximum damage resistance over LVI.

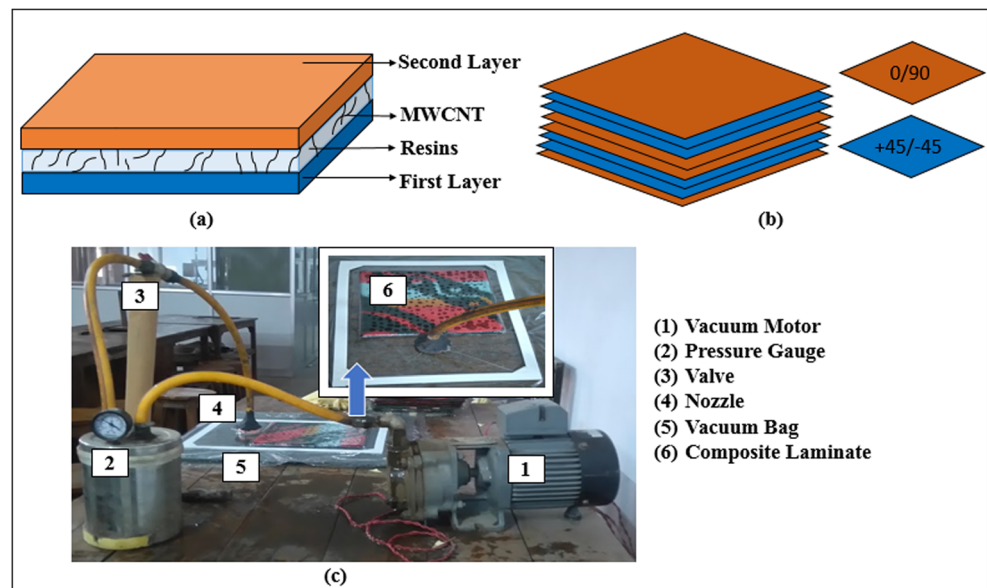
As doping percentage of CNTs in resins grow, the chances of formation of agglomeration increases as the flow of resins happen through the thickness in vacuum bagging method [31, 32]. Several methods have also been discussed for proper dispersion of nanotubes in epoxy to improve rheological behavior [33]. However, above a certain value of nanoparticle doping, agglomeration causes degradation in material performance. Thus it is not preferred to go beyond the certain limit of nano particle reinforcement. The presented review highlighted the unavailability of an optimized value of MWCNTs as secondary reinforcement in carbon woven composite to get maximum damage tolerance over drop weight LVI. For increasing MWCNT doping a hybrid method, i.e., combining hand lay-up technique assisted by vacuum bagging method is adopted. This hybrid technique reduces matrix flow through thickness (as suction occurs in wet laminate only) therefore chances of agglomeration reduced as well. This paper experimentally recommends an optimized value for MWCNT doping in three phased CFRP laminate to attain maximum damage tolerance of three phased composite plates regarding energy absorption and damage tolerance. This is the novelty of proposed investigation.

Experimental

Preparation of CFRP Laminate

Carbon woven fabric with 800 TEX 600 GSM, provided by CFW Enterprises (Delhi, India) is used as primary reinforcement. Pristine multiwall carbon nanotubes (purchased from United Nanotech Innovations Pvt. Ltd., Bangalore, India) is the secondary reinforcing material for three-phased carbon woven composite (Fig. 1(a)). The thickness of the MWCNTs provided is 5–20 nm, 1–10 μm of length with 98% purity. Bisphenol-A (L-12); a thermosetting epoxy N,N'-Bis (2-aminoethyl) ethane-1,2-diamine; a room temperature hardener (K6), purchased from Atul Ltd., Gujrat, India are used as matrix materials. Eight layered quasi-isotropic symmetrical laminate (Fig. 1(b)) with stacking sequence $[(0^0/90^0) / (+45^0/-45^0) / (+45^0/-45^0) / (0^0/90^0) // (0^0/90^0) / (+45^0/-45^0) / (+45^0/-45^0) / (0^0/90^0)]$ is manufactured using hand lay-up

Fig. 1 (a) Three phased composite, (b) Symmetrical laminate design and (c) Vacuum bagging set-up



technique assisted by vacuum bagging at 0.9 atmospheric pressure (Fig. 1(c)) at room temperature. The main reason for the selection of specific layup is that, symmetrical laminate performs better than any other design under low velocity impact loading [10].

In order to manufacture the three-phase composite; woven carbon fabric of dimensions $150 \times 150 \text{ mm}^2$ and fiber orientation of $(0^\circ/90^\circ)$ and $(+45^\circ/-45^\circ)$ are cut. The dispersion of nanotubes in epoxy is a grave concern, and different techniques have been proposed for uniform dispersion of single/multi-wall nanotubes in resins [34]. Therefore, one of the finest available technique which is followed for mixing MWCNTs in resins.

Surface modified procured MWCNTs (using 20% hydrogen peroxide for 45 min) were sonicated (OSCAR-SONOPROS PR-600) with acetone. Then Bisphenol-A, a thermosetting epoxy is added in the solution. Entire system is sonicated for 30 min. Further, magnetic stirring at elevated temperature is done for the complete evaporation of acetone. Hardener K-6 in 10:1 ratio (epoxy: hardener) is mixed and sonicated for 10 min. For avoiding any heat generation during sonication process, system was covered in ice-blanket.

Fabrication of composite laminate is done in two steps initially hand lay-up technique and further application of vacuum bagging method. In the first step, a woven carbon fabric layer $(0^\circ/90^\circ)$ is placed on a flat glass surface, and then two-phased resins are applied using a soft brush. The second layer $(+45^\circ/-45^\circ)$ is placed over first, and resins are applied in a similar means. For removing extra resins, an iron roller was rolled after placing two layers. Extra resins came out from the edges of the woven carbon fabric during rolling. In this way, eight layered wet laminate was prepared according to proposed stacking sequence. For the second step, the prepared wet laminate is kept inside the vacuum bag, and 690 mm of Hg pressure was applied

and kept so for 30 min to squeeze maximum resins through the thickness. Loads of 30 Kg. have been implemented after vacuum pressure was released and curing of the laminate was done for next 24 h at normal temperature pressure. The thickness CFRP composite laminates were $4.0 \pm 0.1 \text{ mm}$, and these samples are scanned using FESEM for void contents and it is observed that void content are negligible.

Drop Weight Testing

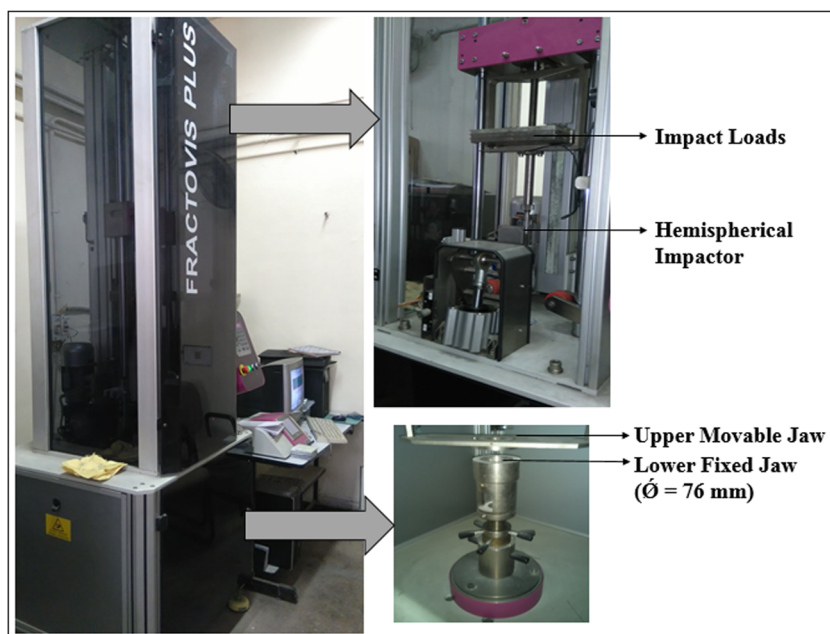
Drop weight impact testing (according to ASTM D7136) is performed on Instron-CEAST 9350 with a hemispherical headed cylindrical impactor of 10 Kg and 12.7 mm diameter. The tests are done by dropping a steel impactor transversely at three different velocities of 3.5, 4.5 and 5.5 m/s. Three specimens of each sample, i.e., neat CFRP (reference material), 1.0, 2.0, 3.0 and 4.0 wt.% of resins were tested. Figure 2 shows the drop weight testing tower and fixtures to mount the CFRP specimen.

Results and Discussion

Energy Absorption

Figure 3 shows the energy-absorbing characteristics for neat and MWCNTs doped samples at three loading velocities. For impact velocity of 3.5 m/s, energy absorption varied with the variation of MWCNT doping percentage. As the impacted energy was not sufficient to penetrate the laminate, impactor rebounding took place and no complete penetration is observed at this velocity. The rebounding of impactor depends on the stiffness of the testing specimen and thus the energy absorption varies with MWCNT doping percentage. Due to the rebounding, swelling or minor fiber fracture opposite to

Fig. 2 Drop weight impact tower



indenter side was seen. Whereas, at 4.5 m/s and 5.5 m/s, complete penetration occurred and maximum energy was absorbed by the specimen with 3 wt.% of the MWCNTs.

Figure 3(a) shows the energy vs. displacement plots at 3.5 m/s impact velocity. At this impact velocity, there is not much variation in energy absorption due to insufficient impact energy. For impact velocity of 4.5 m/s and 5.5 m/s, where complete penetration of CFRP laminate took place witnessed increased energy absorption with the increasing doping value of multiwall carbon nanotubes (Fig. 3(b)). For 4.5 m/s impact velocity energy absorption (EA) improved from 60.6 J (neat CFRP) to 77.4 J at 3 wt.% MWCNTs reinforcement. At 5.5 m/s impact velocity, EA increased from 62.2 J (neat CFRP) to 94.53 J for 3 wt.% doping of MWCNTs in CFRP (Fig. 3(c)).

It had been reported that 50% improvement in energy absorption was possible by using COOH-MWCNTs [25], while the present work confirms that improving reinforcement value of MWCNTs the energy absorption increases till the

agglomeration formation takes place. In addition, 3 wt.% is the optimum doping for mixing value for pristine MWCNTs using a hybrid method, i.e., hand layup technique assisted with vacuum bagging method. Table 1 shows the detailed experimental results of energy absorption.

Load-Time Response

Operational conditions of a composite laminate highly influence the loading conditions as well as damage development in tested specimen [30]. The initial failure of the FRP composite specimen takes place rapidly and occurs within 0.1 milliseconds. Mostly, with an increase in loading on CFRP laminate, its failure initiates from the matrix, which is visible for all incident velocities (Fig. 4(a–c)). The first crack has a tendency to propagate through the thickness of the laminate in transverse loading. However, reinforcement (carbon woven) resists this crack growth in the transverse direction. It is worth

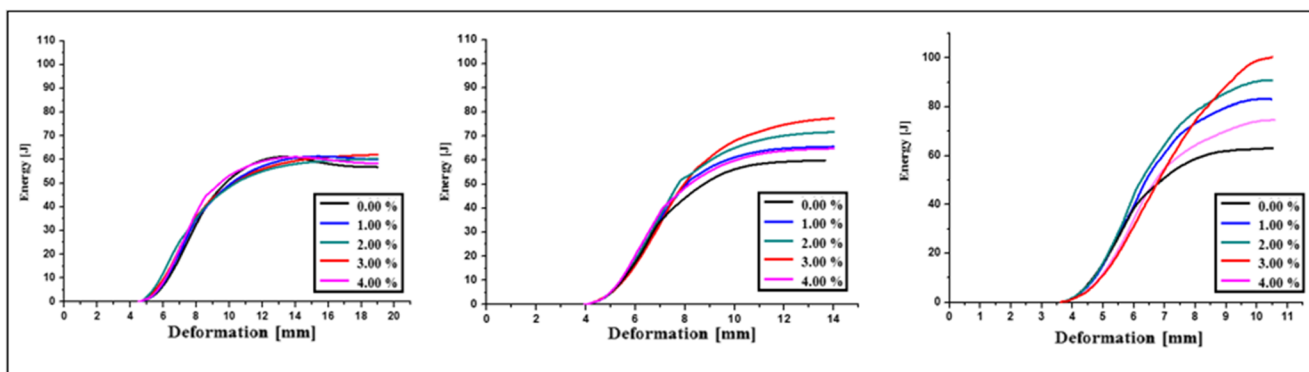
Fig. 3 Energy vs Deformation curves (a) $v = 3.5$ m/s, (b) $v = 4.5$ m/s and (c) 5.5 m/s

Table 1 Energy absorption and Peak Load Values with mean and COV

Neat CFRP	Energy absorption			Peak load		
	3.5 m/s	4.5 m/s	5.5 m/s	3.5 m/s	4.5 m/s	5.5 m/s
Test 1	57.2	59.6	61.2	7891.6	9618.4	9155.2
Test 2	58.6	60.1	62.8	7896.4	9537.89	9230.76
Test 3	55.1	61.7	63	7934.6	9589.1	9354.1
Test 4	54.9	61.2	62.5	7849.1	9548.3	9411.7
Test 5	53.5	60.8	61.8	7921.9	9634.9	9299.1
Mean	55.86	60.6	62.26	7898.72	9585.71	9290.17
COV%	3.61	1.38	1.18	0.41	0.44	1.08
1.0 wt.% MWCNTs						
Test 1	58	62.5	63.7	9511.6	9925.1	9516.2
Test 2	61.3	66.3	66.7	9493.53	10,025.87	9336.02
Test 3	62	69.2	69	9336.1	10,005.2	9216.1
Test 4	59.2	68.9	66.8	9624.1	9862.7	9452.3
Test 5	60.1	67.5	68.1	9211.5	9991.8	9447.1
Mean	60.12	66.88	66.86	9435.36	9962.13	9393.54
COV%	2.66	4.03	2.99	1.71	0.67	1.26
2.0 wt.% MWCNTs						
Test 1	58	69.8	71.5	9512	9994.2	10,135.6
Test 2	61.7	72.3	72	9560.43	10,114.6	10,288.93
Test 3	63	75.1	73	9656.8	9829.4	10,115.5
Test 4	59.6	70.6	71.9	9422.2	10,023.1	9975.2
Test 5	63	73.9	73.4	9537.1	9914.6	10,002.3
Mean	61.06	72.34	72.36	9537.7	9975.18	10,103.5
COV%	3.6	3.04	1.1	0.88	1.08	1.23
3.0 wt.% MWCNTs						
Test 1	65	74.9	93.4	10,756.1	10,954.2	12,012.2
Test 2	62.3	78.2	95.16	10,491.68	11,622.92	11,887.88
Test 3	61	79	95.2	10,025.5	12,015	11,824.3
Test 4	63.5	76.9	94.2	9952.3	11,824.3	10,995.2
Test 5	62.3	78.1	94.7	10,702.9	10,992.8	11,214.2
Mean	62.82	77.42	94.53	10,385.69	11,481.84	11,586.75
COV%	2.38	2.8	0.79	3.62	4.21	3.9
4.0 wt.% MWCNTs						
Test 1	60	62.7	59.6	9198.2	9914.7	7865.2
Test 2	61.5	64.5	62.8	9382.62	9892.79	7699.25
Test 3	62	65.1	63	9514.2	9815.9	7724.5
Test 4	59.9	63.5	60.4	9342.7	9748.2	7624.5
Test 5	62.3	64.7	61.9	9355.7	9963.2	7775.2
Mean	61.14	64.1	61.5	9358.68	9866.95	7737.73
SD	1.12	0.97	1.49	112.66	85.02	89.62
COV%	1.83	1.51	2.42	1.2	0.86	1.15

noticing that both materials; matrix and carbon woven are brittle in nature, with considerable difference in modulus. Due to this modulus difference, FRP delamination, i.e., failure of interfacing takes place. Once load capacity of the woven laminate is reached, it fails and in the meantime, several mechanisms take place simultaneous depending upon the thickness

of the laminate [5]. When MWCNT is used as secondary reinforcement, it delays generation of the first crack as well as it inhibits the crack branching. This results in improvement of load carrying capacity of CFRP composite laminate.

Load-time curves express the maximum load carrying capacity of the specimen including first crack initiation and

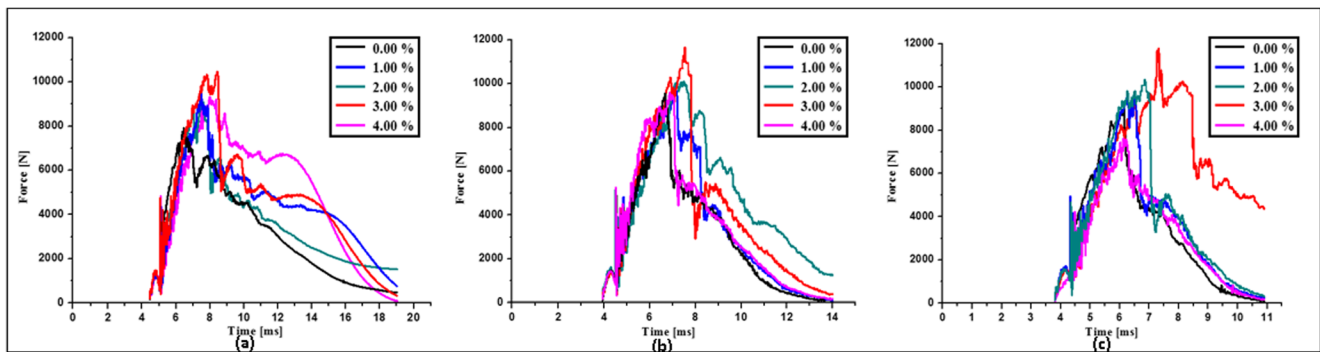


Fig. 4 Load-time curves (a) $v = 3.5$ m/s, (b) $v = 4.5$ m/s and (c) 5.5 m/s

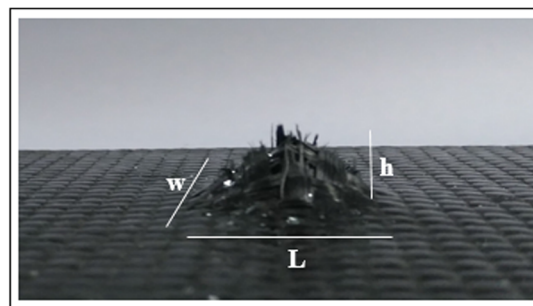
failure behavior of the specimen after peak force is achieved [14]. Figure 4(a) shows rebounding of the impactor as no penetration takes place at 3.5 m/s impact velocity. For incident velocity of 4.5 and 5.5 m/s shown in Fig. 4(b–c), impactor penetrated the laminate and maximum peak force was observed at 3 wt.% of MWCNT doping. With the increase in incident velocity, load capacity seems to be increasing, but the maximum load value is detected for 3 wt.% of doping.

Figure 4 also explains that damage mechanism like matrix-cracking dominates primarily at the lower end of the force-time curve. While mechanism like peak load capacity occurred at the velocity of the central section of the curve and lastly, delamination and ply shearing occurred once peak force is reached these mechanisms are seen for complete penetration of CFRP laminate, i.e., in Fig. 4(b–c). Table 1 shows the detailed experimental results of load capacity.

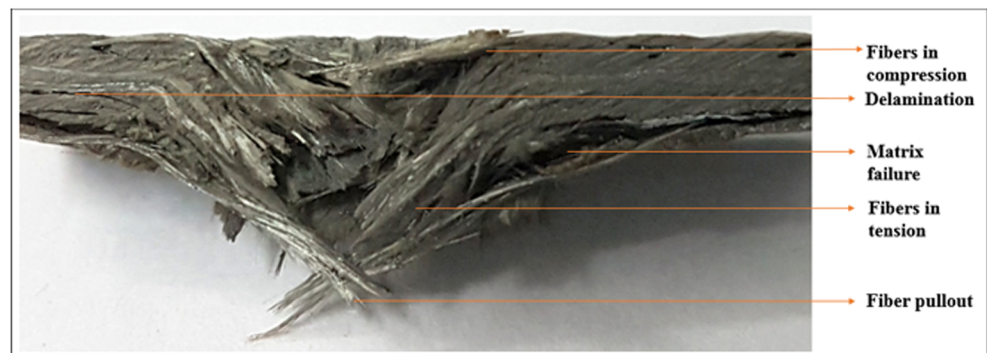
Pyramidal Damage

Impactor shape affects the damage pattern as well as damage area [35]. Therefore in this section, pyramidal damage area caused by hemispherical impactor is calculated. It can be realized that crushing of top layer starts very soon after impact loading starts. The top surface of the CFRP laminate undergoes compression while bottom layer experiences tensile failure [36]. Hemispherical impactor causes maximum stress at the tip of the indenter, i.e., maximum load is at the center of the impact. For a thin-ply laminate, compressive and tensile loading occurred resulting in a pyramidal pattern of damage. The pattern of the pyramidal damage is represented in Fig. 5(a–b) as the cross-sectional view of the damaged specimen (FRP).

Fig. 5 (a) Pyramidal damage. (b) Cross-section view of damage zone



(a)



(b)

Table 2 Damage area comparison for CFRP laminates (mean values)

Velocity of impact Doping Wt. %	3.5 m/s		4.5 m/s		5.5 m/s	
	Rectangular area (mm ²)	Height (h)	Rectangular area (mm ²)	Height (h)	Rectangular area (mm ²)	Height (h)
Neat	173.43	5.2	242.45	7.0	354.50	12.0
1.0%	152.75	5.0	232.77	6.5	312.47	12.1
2.0%	146.00	5.1	219.41	5.8	265.09	11.9
3.0%	Negligible	Swelling	206.77	5.0	242.06	11.0
4.0%	61.21	3.0	228.15	9.0	326.96	13.5

To calculate the visible damage area, the rectangular area of damage (damage in warp and weft direction) and pyramid height are measured and compared. It is observed that minimum damage area is found in for 3 wt.% doping while maximum damage area is calculated for 4 wt.% reinforcement of multiwall carbon nanotubes. Table 2 represents the damaged area for proposed neat and MWCNT embedded specimens. It is evident that for all impact velocities (3.5, 4.5 and 5.5 m/s) and doping values, the visible damage is minimum at 3 wt.% of MWCNTs in resin.

FESEM Analysis

Problem-related to resin flow in vacuum bagging method has been already discussed in the introduction. Field emission scanning electron microscopy (FESEM) is done to analyze MWCNTs agglomeration. Figure 6(a–f) shows the

interactions between matrix and reinforcement in MWCNT embedded CFRP laminates. Cross-section scanning of prepared composite clarifies the MWCNT agglomeration presence at 4 wt% reinforcement. This agglomeration reduced the energy absorption. Therefore higher damage area is also observed as compared to other specimens at lower doping percentage.

Carbon nanotube distribution in the fabricated laminates differ from those in neat matrix. Dual scale behavior by CNT/epoxy mixture leads to screening effect, which sieves most of the nanoparticles within the layers of fiber weave. Nanotube alignments within CNT modified laminates very much controls their overall response towards applied load/force. In addition, implied manufacturing process dictates the alignment of these nanoparticles. Hybrid laminate manufacturing process (hand layup followed by vacuum bagging method) helped retain the dispersion status of the CNT in

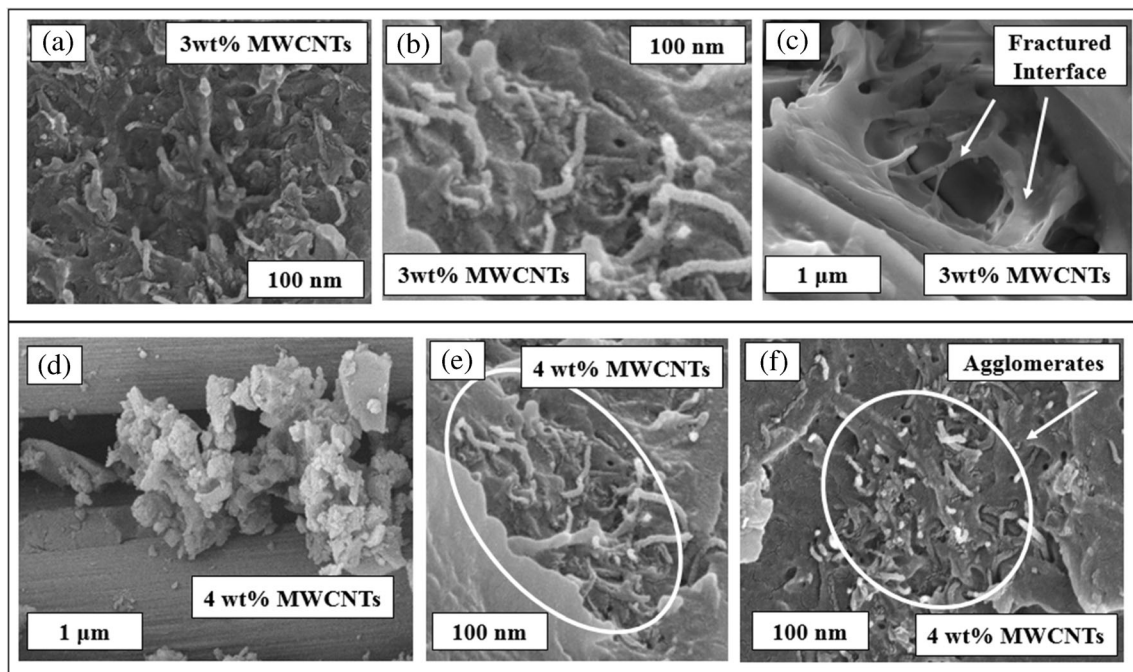


Fig. 6 (a–b) Uniform dispersion of MWCNTs at 3 wt.%, (c) Interaction of MWCNTs and resins after fracture, (d–f) Agglomeration of MWCNTs in matrix system

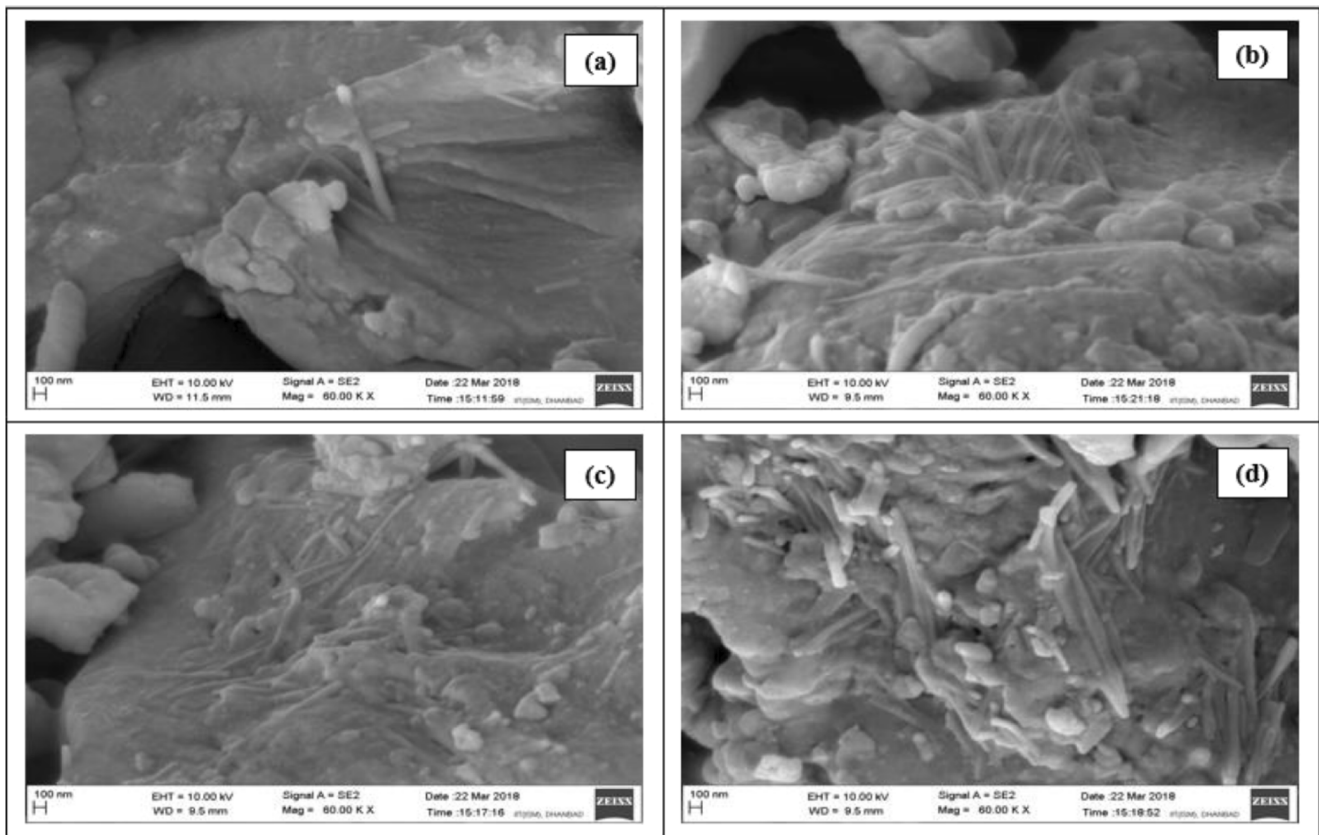


Fig. 7 Dispersion state of MWCNTs in bulk matrix (in-situ polymerized) (a) 1.0 wt.%, (b) 2.0 wt.%, (c) 3.0 wt.% and (d) 4.0 wt.% respectively

between the plies. Although, vacuum (equivalent to 690 mm of Hg) implemented during the fabrication process aligned the MWCNTs in resin flow direction, which improved interlaminar properties of the specimens. Figure 7(a–d) shows nanotubes alignment within the three-phased FRP specimen with increasing concentration (1 to 4 wt.% respectively).

Internal Damage

In low-velocity impact situation, internal damage is barely visible and hard to detect. Internal damage includes matrix failure as, cracking and delamination inside laminate plate. Internal damage reduces the component performance, and

increases lead to catastrophic accidents. In this paper scanning acoustic microscopy (SAM) is done to analyze the internal damage. The KSI scanning acoustic v-400 series microscope is used to scan 4 mm thick specimen. The thickness of the specimen is divided into eight layers for scanning, and then the maximum damage is considered for evaluation and comparison. The comparison of SAM images validates damage results, i.e., maximum damage is visible for 4 wt% reinforcement while at 3 wt% of doping minimum circular damage is found. The main reason for increased damage at high doping percentage is MWCNT agglomeration (Fig. 8) which causes interfacial failure. Thus, highest damage is visible for 4 wt% reinforcement.

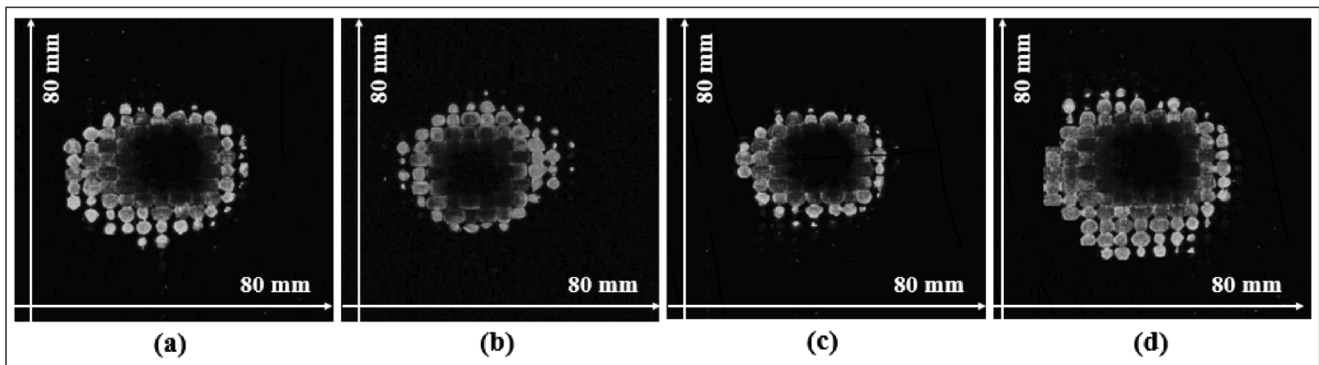


Fig. 8 SAM analysis (a) Neat sample, (b) 2 wt% doping, (c) 3 wt% doping and (d) 4 wt% doping

Conclusion

In this study, experimental investigation of three-phased carbon woven/epoxy composite laminate over drop weight impact test is done. Increase in impact resistance with doping percentage has been perceived while after a certain value property of the laminate start decreasing. Therefore, an optimum value for maximum impact resistance has been proposed for LVI test using a hemispherical impactor. Findings of this paper can be summarized as:

- Doping of multiwall carbon nanotubes in the matrix (resins) as secondary reinforcement enhances energy absorption property in carbon woven/MWCNT/epoxy composite.
- Maximum energy absorption value is attained at 3 wt% reinforcement meanwhile the optimum value of MWCNT doping is 3 wt% of resins and at 5.5 m/s velocity energy absorption is increased by 51.83%.
- Maximum load capacity is also attained for optimum doping value, i.e., 3 wt% reinforcement of MWCNT in resins.
- Reinforcement of multiwall carbon nanotube influences pyramidal damage area (visible) and internal damage area (barely visible) as well. It is calculated that for 3 wt% reinforcement both damaged areas are minimum while above this doping value damage area increases.

References

1. Eydani M, Niezrecki C, Sherwood J, Avitabile P (2016) Shock & vibration, aircraft/aerospace, energy harvesting, acoustics & optics, vol 9
2. Asl ME, Niezrecki C, Sherwood J, Avitabile P Similarity analysis of composite I-beams with application to subcomponent testing of wind turbine blades. *Experimental and Applied Mechanics* 4:115–126. https://doi.org/10.1007/978-3-319-22449-7_14
3. Handschuh KM, Miller GS, Sinnott MJ, Kohlman LW, Roberts GD, Pereira JM, Ruggeri RC (2015) Society for the advancement of materials and process engineering. Covina, CA, United States
4. Agrawal S, Singh KK, Sarkar PK Impact damage on fibre-reinforced polymer matrix composite – A review. *J Compos Mater* 48(3):317–332. <https://doi.org/10.1177/0021998312472217>
5. Hufenbach W, Ibrahim FM, Langkamp A, Böhm R, Hornig A (2008) Charpy impact tests on composite structures – an experimental and numerical investigation. *Compos Sci Technol* 68:2391–2400. <https://doi.org/10.1016/j.compscitech.2007.10.008>
6. Schweizerhof TRK, Weimar K, Münz T (1998) 5th Int. LS-DYNA Users Conf. Southfield, Michigan
7. Rawat P, Singh KK (2017) An impact behavior analysis of CNT-based fiber reinforced composites validated by LS-DYNA: a review. *Polym Compos* 38:175–184. <https://doi.org/10.1002/pc.23573>
8. S R Reid ZZ (2000) Impact behaviour of fibre-reinforced composite materials and structures. Woodhead Publishing Ltd. and CRC Press LLC
9. Singh KK, Singh RK, Chandel PS, Kumar P (2008) An asymmetric FRP laminate with a circular precrack to determine impact-induced damage. *Polym Compos* 29:1378–1383. <https://doi.org/10.1002/pc.20422>
10. Singh KK, Singh NK, Jha R (2016) Analysis of symmetric and asymmetric glass fiber reinforced plastic laminates subjected to low-velocity impact. *J Compos Mater* 50:1853–1863. <https://doi.org/10.1177/0021998315596594>
11. Singh NK, Rawat P, Singh KK (2016) Impact response of quasi-isotropic asymmetric carbon fabric/epoxy laminate infused with MWCNTs. *Adv Mater Sci Eng* 2016:1–7. <https://doi.org/10.1155/2016/7541468>
12. Angrizani CC, Cioffi MO, Zattera AJ, Amico SC (2014) Analysis of curaua/glass hybrid interlayer laminates. *J Reinf Plast Compos* 33:472–478. <https://doi.org/10.1177/0731684413517519>
13. Pandya KS, Pothnis JR, Ravikumar G, Naik NK (2013) Ballistic impact behavior of hybrid composites. *Mater Des* 44:128–135. <https://doi.org/10.1016/j.matdes.2012.07.044>
14. Hosur MV, Abdullah M, Jeelani S (2005) Studies on the low-velocity impact response of woven hybrid composites. *Compos Struct* 67(3):253–262. <https://doi.org/10.1016/j.compstruct.2004.07.024>
15. Richardson MOW, Wisheart MJ (1996) Review of low-velocity impact properties of composite materials. *Compos A: Appl Sci Manuf* 27(12):1123–1131. [https://doi.org/10.1016/1359-835X\(96\)00074-7](https://doi.org/10.1016/1359-835X(96)00074-7)
16. Wang H, Ramakrishnan KR, Shankar K (2016) Experimental study of the medium velocity impact response of sandwich panels with different cores. *Mater Des* 99:68–82. <https://doi.org/10.1016/j.matdes.2016.03.048>
17. Wang J, Chen B, Wang H, Waas AM (2015) Experimental study on the compression-after-impact behavior of foam-core sandwich panels. *J Sandw Struct Mater* 17:446–465. <https://doi.org/10.1177/1099636215577367>
18. Ashrafi B, Guan J, Mirjalili V, Zhang Y, Chun L, Hubert P, Simard B, Kingston CT, Bourne O, Johnston A (2011) Enhancement of mechanical performance of epoxy/carbon fiber laminate composites using single-walled carbon nanotubes. *Compos Sci Technol* 71:1569–1578. <https://doi.org/10.1016/j.compscitech.2011.06.015>
19. Koricho EG, Khomenko A, Haq M, Drzal LT, Belingardi G, Martorana B (2015) Effect of hybrid (micro- and nano-) fillers on impact response of GFRP composite. *Compos Struct* 134:789–798. <https://doi.org/10.1016/j.compstruct.2015.08.106>
20. Kostopoulos V, Baltopoulos A, Karapappas P, Vavouliotis A, Paipetis A (2010) Impact and after-impact properties of carbon fibre reinforced composites enhanced with multi-wall carbon nanotubes. *Compos Sci Technol* 70:553–563. <https://doi.org/10.1016/j.compscitech.2009.11.023>
21. Iijima S (1991) Helical microtubules of graphitic carbon. *Nature* 354:56–58. <https://doi.org/10.1038/354056a0>
22. Schadler LS, Giannaris SC, Ajayan PM (1998) Load transfer in carbon nanotube epoxy composites. *Appl Phys Lett* 73:3842–3844. <https://doi.org/10.1063/1.122911>
23. Karapappas P, Vavouliotis A, Tsotra P, Kostopoulos V, Paipetis A (2009) Enhanced fracture properties of carbon reinforced composites by the addition of multi-wall carbon nanotubes. *J Compos Mater* 43:977–985. <https://doi.org/10.1177/0021998308097735>
24. Davis DC, Wilkerson JW, Zhu J, Hadjiev VG (2011) A strategy for improving mechanical properties of a fiber reinforced epoxy composite using functionalized carbon nanotubes. *Compos Sci Technol* 71:1089–1097. <https://doi.org/10.1016/j.compscitech.2011.03.014>
25. Hull D, Shi YB (1993) Damage mechanism characterization in composite damage tolerance investigations. *Compos Struct* 23:99–120. [https://doi.org/10.1016/0263-8223\(93\)90015-I](https://doi.org/10.1016/0263-8223(93)90015-I)
26. Siegfried M, Tola C, Claes M, Lomov SV, Verpoest I, Gorbatiikh L (2014) Impact and residual after impact properties of carbon fiber/

- epoxy composites modified with carbon nanotubes. *Compos Struct* 111:488–496. <https://doi.org/10.1016/j.compstruct.2014.01.035>
27. Koricho EG, Khomenko A, Haq M, Drzal LT, Belingardi G, Martorana B (2015) Effect of hybrid (micro- and nano-) fillers on impact response of GFRP composite. *Compos Struct* 134:789–798. <https://doi.org/10.1016/j.compstruct.2015.08.106>
 28. Garcia-Gonzalez D, Rodriguez-Millan M, Rusinek A, Arias A (2015) Investigation of mechanical impact behavior of short carbon-fiber-reinforced PEEK composites. *Compos Struct* 133:1116–1126. <https://doi.org/10.1016/j.compstruct.2015.08.028>
 29. Tehrani M, Boroujeni AY, Hartman TB, Haugh TP, Case SW, Al-Haik MS (2013) Mechanical characterization and impact damage assessment of a woven carbon fiber reinforced carbon nanotube-epoxy composite. *Compos Sci Technol* 75:42–48. <https://doi.org/10.1016/j.compscitech.2012.12.005>
 30. Soliman EM, Sheyka MP, Taha MR (2012) Low-velocity impact of thin woven carbon fabric composites incorporating multi-walled carbon nanotubes. *Int J Impact Eng* 47:39–47. <https://doi.org/10.1016/j.ijimpeng.2012.03.002>
 31. Gojny FH, Wichmann MHG, Fiedler B, Bauhofer W, Schulte K (2005) Influence of nano-modification on the mechanical and electrical properties of conventional fibre-reinforced composites. *Compos Part A Appl Sci Manuf* 36:1525–1535. <https://doi.org/10.1016/j.compositesa.2005.02.007>
 32. Rachmadini Y, Tan VBC, Tay TE (2010) Enhancement of mechanical properties of composites through incorporation of CNT in VARTM - a review. *J Reinf Plast Compos* 29:2782–2807. <https://doi.org/10.1177/0731684409359103>
 33. Song YS, Youn JR (2005) Influence of dispersion states of carbon nanotubes on physical properties of epoxy nanocomposites. *Carbon* N Y 43:1378–1385. <https://doi.org/10.1016/j.carbon.2005.01.007>
 34. Ma P-C, Siddiqui NA, Marom G, Kim J-K (2010) Dispersion and functionalization of carbon nanotubes for polymer-based nanocomposites: a review. *Compos Part A Appl Sci Manuf* 41:1345–1367. <https://doi.org/10.1016/j.compositesa.2010.07.003>
 35. Sevkat E, Liaw B, Delale F (2013) Drop-weight impact response of hybrid composites impacted by impactor of various geometries. *Mater Des* 52:67–77. <https://doi.org/10.1016/j.matdes.2013.05.016>
 36. Silberschmidt V (2016) *Dynamic deformation, damage and fracture in composite materials and structures* 1st Edition. Woodhead Publishing Ltd

Publisher's Note Springer Nature remains neutral with regard to jurisdictional claims in published maps and institutional affiliations.

